



Excitation cross section of erbium-doped GaN waveguides under 980 nm optical pumping

R. Hui, R. Xie, I.-W. Feng, Z. Y. Sun, J. Y. Lin, and H. X. Jiang

Citation: [Applied Physics Letters](#) **105**, 051106 (2014); doi: 10.1063/1.4892427

View online: <http://dx.doi.org/10.1063/1.4892427>

View Table of Contents: <http://scitation.aip.org/content/aip/journal/apl/105/5?ver=pdfcov>

Published by the [AIP Publishing](#)

Articles you may be interested in

[Emission and absorption cross-sections of an Er:GaN waveguide prepared with metal organic chemical vapor deposition](#)

Appl. Phys. Lett. **99**, 121106 (2011); 10.1063/1.3636418

[Carrier lifetime in erbium-doped GaN waveguide emitting in 1540 nm wavelength](#)

Appl. Phys. Lett. **97**, 241105 (2010); 10.1063/1.3527089

[Erbium-doped GaN optical amplifiers operating at 1.54 \$\mu\text{m}\$](#)

Appl. Phys. Lett. **95**, 111109 (2009); 10.1063/1.3224203

[Absorption cross section and signal enhancement in Er-doped Si nanocluster rib-loaded waveguides](#)

Appl. Phys. Lett. **86**, 261103 (2005); 10.1063/1.1957112

[Optical gain in optically pumped cubic GaN at room temperature](#)

Appl. Phys. Lett. **70**, 1076 (1997); 10.1063/1.118489

The logo for AIP APL Photonics is displayed in white text on a red background. The background features a bright yellow sunburst effect in the upper right corner.

AIP | APL Photonics

APL Photonics is pleased to announce
Benjamin Eggleton as its Editor-in-Chief



Excitation cross section of erbium-doped GaN waveguides under 980 nm optical pumping

R. Hui,¹ R. Xie,¹ I.-W. Feng,² Z. Y. Sun,² J. Y. Lin,² and H. X. Jiang²

¹Department of Electrical Engineering and Computer Science, The University of Kansas, Lawrence, Kansas 66045, USA

²Department of Electrical and Computer Engineering, Texas Tech University, Lubbock, Texas 79409, USA

(Received 28 June 2014; accepted 25 July 2014; published online 5 August 2014)

Excitation cross section of erbium-doped GaN waveguides is measured to be approximately $2.2 \times 10^{-21} \text{ cm}^2$ at 980 nm pumping wavelength. This cross section value is found relatively insensitive to the crystalline quality of epilayers. However, spontaneous emission carrier lifetimes in these waveguides are directly related to both the crystalline quality and the optical loss, and thus can be used as a material quality indicator. © 2014 AIP Publishing LLC.

[<http://dx.doi.org/10.1063/1.4892427>]

Doped in a solid host, erbium ion allows intra 4f shell transition from its first excited state ($^4I_{13/2}$) to the ground state ($^4I_{15/2}$), corresponding to an emission wavelength in the 1550 nm band which is within the minimum loss window of optic fibers used in communication systems.^{1–3} Thus, Er-doped materials are ideal candidates to make optical amplifiers for fiber-optic communications, known as Er-doped fiber amplifiers (EDFAs). On the other hand, optical amplification in photonic integrated circuits requires materials with much higher gain per unit length, and suitable for monolithic integration. Travelling-wave semiconductor optical amplifiers (SOAs)⁴ based on InGaAsP are integratable with other components such as laser sources in III–V material platform. However, due to the short carrier lifetime of typically less than a nanosecond, cross-saturation in an SOA may cause significant inter-channel crosstalk between different wavelength channels, which to a large extent prevented SOA from being used in wavelength division multiplexed (WDM) optical systems.⁵

III-nitride wide bandgap semiconductors are excellent host materials for erbium ions due to their structural and thermal stabilities. Monolithic growth of III-nitride semiconductor on silicon substrate has also been demonstrated,^{6,7} which opens the possibility of integrated optical amplifiers in silicon photonics based on erbium-doped III-nitride. Photoluminescence^{8–10} and optical amplification¹¹ in 1.54 μm wavelength window have been demonstrated in waveguides based on Er-doped GaN and AlGaIn epilayers at room temperature. The mechanism of erbium ion excitation depends on the wavelength of optical pumping source. Above-bandgap pumping at UV wavelength excites free electrons and holes in the semiconductor host material, and subsequently the electrons and holes transfer their energy to the doped erbium ions to produce carrier population on the $^4I_{13/2}$ band which is responsible for emission and amplification in the 1.54 μm wavelength window. Whereas, below-bandgap pumping using wavelengths below GaN bandgap resonantly excites erbium ions without interacting with the band structure of the host semiconductor material. Excitation cross section is a key parameter which determines the efficiency of optical pumping. Above-bandgap excitation with 350 nm wavelength could be several orders more efficient than below-bandgap excitation with 1480 nm,¹² however, most of the commercial EDFAs are

pumped by 980 nm diode lasers thanks to the wide availability of high power semiconductor laser sources in this wavelength window. Practical application of optical amplifiers based on erbium-doped GaN (Er:GaN) will thus conceivably rely on 980 nm pumping. The crystalline quality of an Er:GaN optical waveguide is critical, which determines several key parameters including optical loss, carrier lifetime, as well as the efficiency of photon emission. Linear relation was found between optical attenuation coefficient of Er:GaN waveguide and the x-ray rocking curve linewidth of the GaN crystal.¹³ In this Letter, we show that spontaneous emission carrier lifetime is inversely proportional to the x-ray rocking curve linewidth. In addition, we show that the excitation cross section of Er:GaN at 980 nm wavelength is approximately $2.2 \times 10^{-21} \text{ cm}^2$, which is relatively independent of the Er:GaN crystalline quality.

The Er:GaN epilayers were synthesized by metal organic chemical vapor deposition (MOCVD) in a horizontal reactor. Trimethylgallium was used for the Ga source, and NH_3 was used as the N source. The metalorganic precursor used for the in-situ Er doping was Tris(2,2,6,6-tetramethyl-3,5-heptanedionato) erbium, which was transported to the reactor by H_2 . All samples were grown on (0001) sapphire substrates. Three Er:GaN waveguides with a similar Er concentration of approximately $2 \times 10^{20} \text{ cm}^{-3}$ (Ref. 13) were used in this study with their layer structures shown in the inset of Fig. 1. Using Al-rich AlGaIn or AlN as the cladding layers of Er:GaN waveguides offers an adjustable index contrast between the core and cladding and thus a controllable lever of optical confinement. However, the strain induced by the lattice mismatch between Er:GaN core and AlGaIn or AlN claddings may also introduce a degradation in Er:GaN crystalline quality. This crystalline quality can be quantified by an x-ray diffraction (XRD) measurement. The full-width at half maximum (FWHM) of XRD rocking curves of (002) peak (ω -scan) are 430, 530, and 650 arc-seconds, respectively, for samples A, B, and C.¹³ As a comparison, the undoped GaN epilayers grown on sapphire synthesized with the same MOCVD system typically have a FWHM of approximately 360 arc sec for (002) racking curve. The quantitative measure of crystalline quality allows the investigation of its impact in other parameters of Er:GaN waveguides.

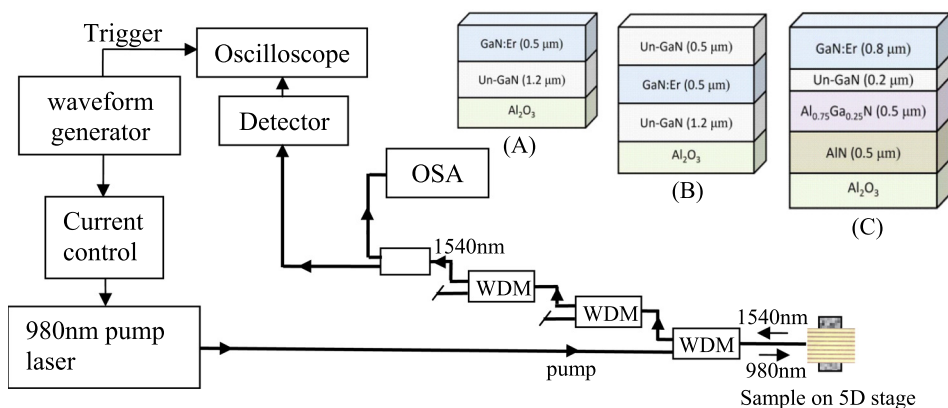


FIG. 1. Experimental setup. Inset shows layer structures of three waveguide samples.

Fig. 1 shows the block diagram of experimental setup used to characterize the Er:GaN waveguide samples. A 980 nm laser diode with single-mode fiber pigtail is used as the pump source. The injection current is controlled by an arbitrary waveform generator which creates square-wave pulses with programmable pulse widths and amplitudes. The optical power from the pump is coupled into one end of an Er:GaN waveguide through a 980 nm/1550 nm WDM coupler and a single-mode fiber with a lensed end-facet for focusing. This lensed fiber terminal has a focal diameter of approximately $2.5 \mu\text{m}$. With 980 nm optical pump coupled into the waveguide, backward propagated spontaneous emission at 1540 nm wavelength is generated which is collected by the same lensed fiber terminal.¹⁴ Three identical 980 nm/1550 nm WDM couplers are used in the system, each having approximately 20 dB isolation between 980 nm and 1540 nm wavelength components. These WDM couplers ensure that 980 nm pump power reflected from the end facet of the waveguide is not received by the photo-detector and the optical spectrum analyzer (OSA). Optical loss values of these three waveguides have been measured previously which are 6 dB/cm, 14 dB/cm, and 43 dB/cm, respectively. It has also been found that the optical attenuations of waveguides depend on the quality of the GaN crystalline quality characterized by the FWHM of XRD rocking curves.¹³ Higher

optical loss was found to be associated with broader XRD rocking curves. In general, optical loss in a waveguide can be attributed to both scattering and absorption of optical signal. While scattering depends on the optical structures with feature sizes comparable to the wavelength of the optical signal, absorption is often related to non-radiative recombination of carriers induced by crystalline disordering with much smaller feature sizes.

As the quality of Er:GaN crystalline has an important impact in the carrier recombination process, its impact in the spontaneous emission lifetime, τ_e , should also be expected. τ_e is related to both radiative recombination and non-radiative recombination, and therefore it is an important indication of crystalline quality, particularly in the microscopic levels. Fig. 2(a) shows the transient waveforms of 1540 nm spontaneous emission measured after the 980 nm pump optical power switches off at $t = 0$. Best fitting to an exponential decay indicates that the carrier lifetimes are 2.6 ms, 2.3 ms, and 1.1 ms, respectively, for waveguide samples (A), (B), and (C) illustrated in Fig. 1. Fig. 2(b) shows the carrier lifetime and the optical loss as the function of the XRD linewidth. It is evident that reducing XRD linewidth increases the spontaneous emission carrier lifetime. In other words, carrier lifetime is also a direct indication of crystalline quality.

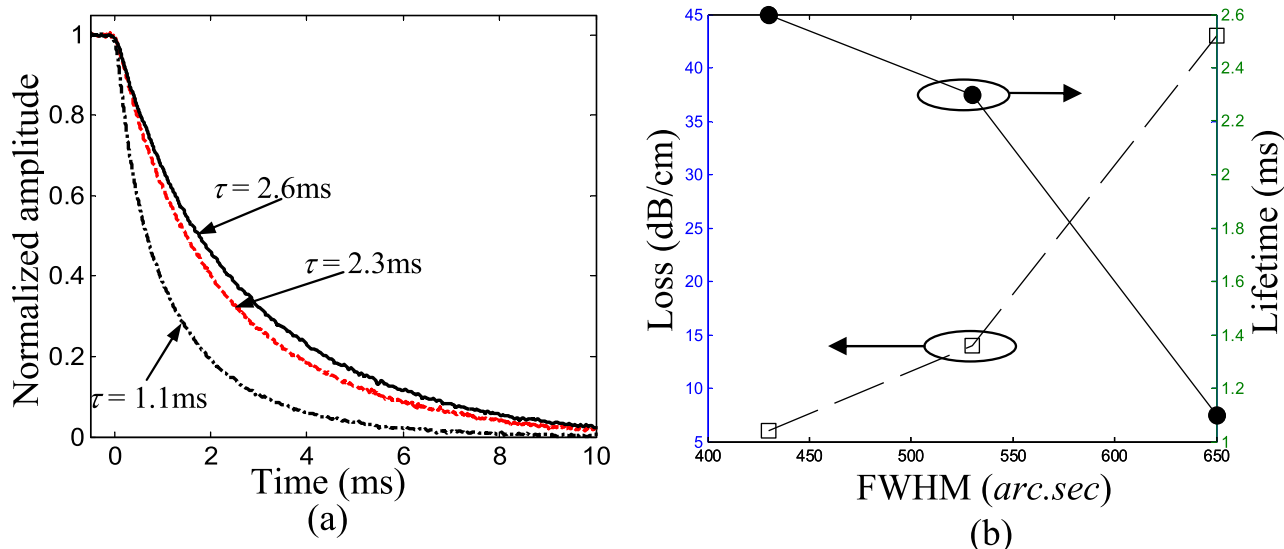


FIG. 2. (a) Measured 1540 nm emission at the falling edge of a pump pulse for samples A (solid line), B (dashed line), and C (dash-dotted line), respectively. (b) Optical loss (open square) and carrier lifetime (circles) as the function of XRD linewidth.

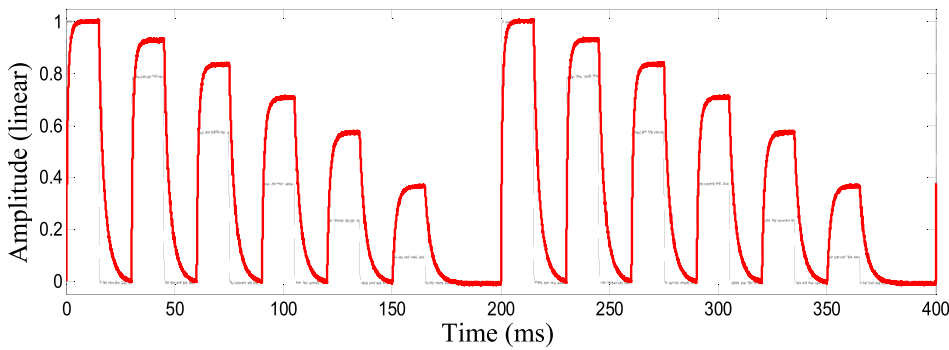


FIG. 3. Normalized 980 nm excitation (dashed) and 1540 nm emission (bold) waveforms of programmed multiple pulses with decreasing amplitude.

In a simplified 2-level system,¹ the carrier density rate equation of Er ions is $dN_2/dt = \sigma_{exc}\varphi_{exc}(N_T - N_2) - N_2/\tau_e$, where, N_2 is the carrier density on the excited $^4I_{13/2}$ state, N_T is the total doping density of erbium atoms, σ_{exc} is the excitation cross section of erbium ions at 980 nm pumping wavelength, and φ_{exc} is the excitation photon flux. If the excitation is applied as a square wave, the response of the 1540 nm emission can be measured at the leading edge and the falling edge of the excitation pulse as shown in Fig. 3. At the falling edge, the excitation pulse is off, and the emission lifetime, τ_e , during the falling edge transition is thus independent of the pump power. However, excitation is “on” in the transition of leading edge, and therefore the effective lifetime $\tau_{eff} = (\sigma_{exc}\varphi_{exc} + 1/\tau_e)^{-1}$ also depends on the level of excitation.¹⁵ Fig. 3 shows normalized waveforms of 980 nm excitation and 1540 nm emission measured with sample (A) using experimental setup shown in Fig. 1. In order to systematically evaluate the carrier lifetime as the function of excitation photon flux, an amplitude-decreasing excitation pulse train is programmed with an arbitrary waveform generator, shown as dashed line in Fig. 3. The corresponding 1540 nm emission waveform is also shown in Fig. 3 as the solid line for comparison. The rise and fall times of the 980 nm excitation pulse are both less than 0.09 ms determined by the time responses of the pump laser and the driving electronic circuits, while the rise and the fall times of the 1540 nm emission are much longer. The rapid scan of the

excitation amplitude avoided possible measurement errors due to variations in optical coupling if pump optical power was manually adjusted.

The solid squares in Fig. 4(a) show the amplitude of 1540 nm emission as the function of the 980 nm excitation flux based on the response shown in Fig. 3. The excitation photon flux value in the horizontal axis of Fig. 4(a) is linearly proportional to the pump optical power, and the conversion between them had included the following factors: (1) the coupling efficiency from the lensed fiber terminal (with a 2.5 μm focal diameter) to the waveguide fundamental mode is about 18.5%, which is the overlap factor between the waveguide fundamental mode and the Gaussian profile of the excitation field at the focal point of the lensed fiber, and (2) the overlap between the waveguide fundamental mode and the Er-doped region of the waveguide cross section is approximately 40%. Assume the waveguide attenuation parameter is α , and the waveguide length is L , the backward propagated 1540 nm emission power collected by the lensed fiber is

$$P_{emit} = \eta \int_0^L \frac{\tau_e \varphi_{exc} e^{-2\alpha z} dz}{1 + \tau_e \sigma_{exc} \varphi_{exc} e^{-\alpha z}} = \frac{\eta}{\alpha \sigma_{exc}} \left[1 - e^{-\alpha L} - \frac{1}{\tau_e \varphi_{exc} \sigma_{exc}} \ln \left(\frac{1 + \tau_e \varphi_{exc} \sigma_{exc}}{1 + \tau_e \varphi_{exc} \sigma_{exc} e^{-\alpha L}} \right) \right], \quad (1)$$

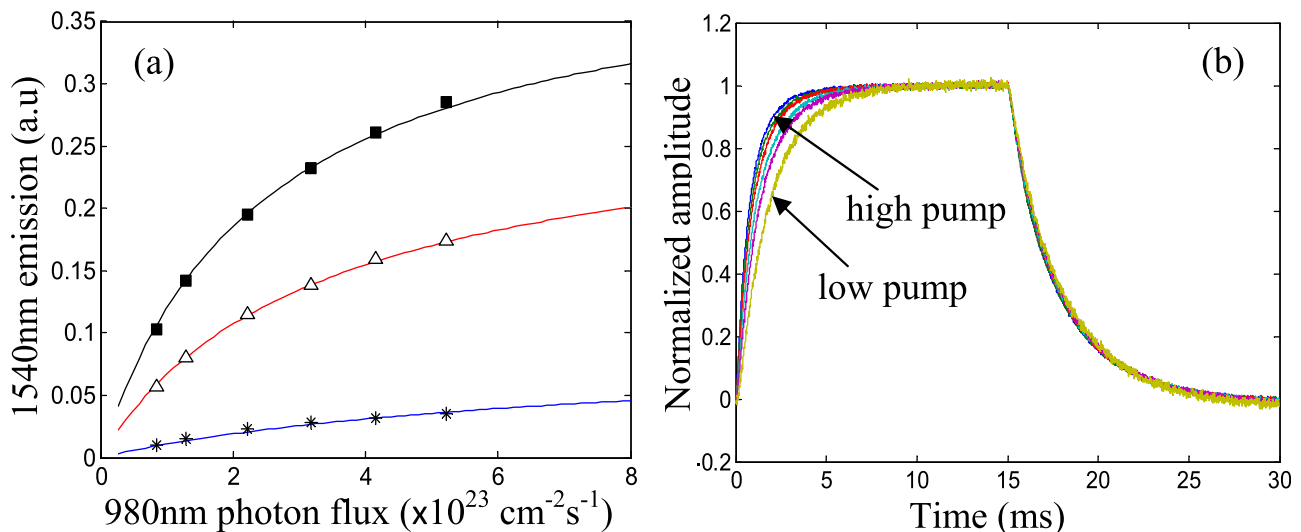


FIG. 4. (a) 1540 nm emission as the function of the excitation photon flux for samples A (solid squares), B (open triangles), and C (stars), respectively, and (b) emission waveforms of sample A after all pulses re-aligned and normalized.

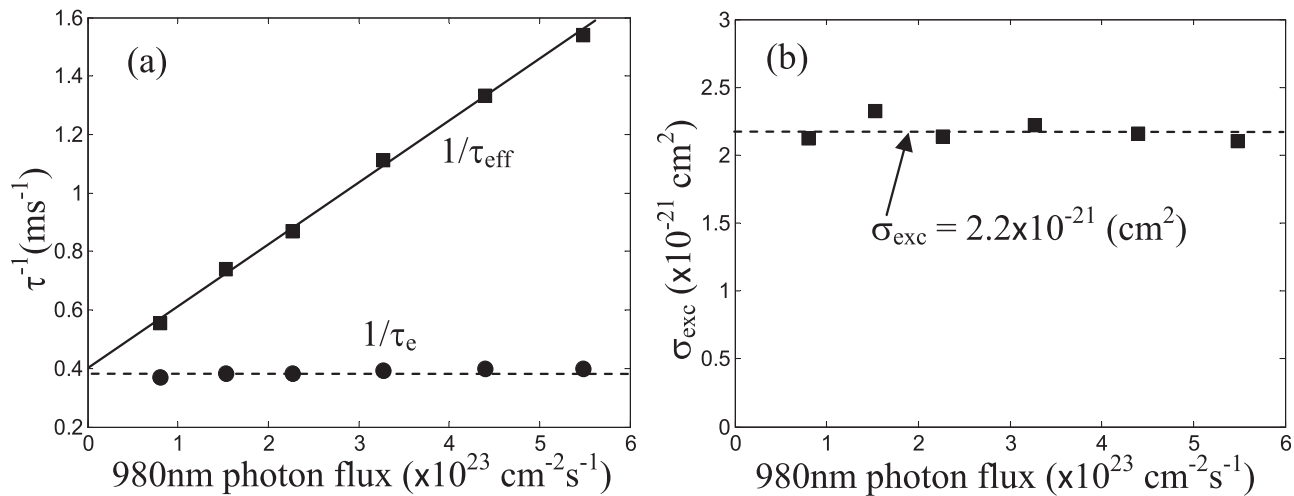


FIG. 5. (a) Measured pulse rise (squares) and fall (circles) time constants of sample A as the function of excitation photon flux. (b) Excitation cross-section derived from the measurement.

where η is a proportionality factor depending on the coupling efficiency between the fiber and the Er-doped region of the waveguide.

In order to compare the detailed waveforms of 1540 nm emission pulses with different excitation levels shown in Fig. 3, we re-align (in time) and re-normalize (in amplitude) all the six pulses in each period and plot them together in Fig. 4(b). As expected, time constant at the pulse falling edge, τ_{e} , is independent of the excitation photon flux, whereas the effective time constant at the pulse leading edge, τ_{eff} , reduces with the increase of excitation photon flux. Fig. 5(a) shows the inverse of rise and fall time constants as a function of excitation photon flux. The slope $d\tau_{\text{eff}}^{-1}/d\phi_{\text{exc}}$ provides the excitation cross-section, σ_{exc} , of the erbium ions at 980 nm pumping wavelength as shown in Fig. 5(b), and the average value is $2.2 \times 10^{-21} \text{ cm}^2$.

We have also measured the amplitude of 1540 nm emission as the function of 980 nm excitation flux for higher loss samples (B) and (C), shown as triangles and stars in Fig. 4(a) for comparison. The continuous lines in Fig. 4(a) were calculated with Eq. (1) for all the three samples based on their respective τ_{e} and α values, while the same excitation cross section value $\sigma_{\text{exc}} = 2.2 \times 10^{-21} \text{ cm}^2$ was used for all the three curves. Waveguides with higher losses produce lower 1540 nm emission. However, the reasonably good agreement between the measured and the calculated saturation characteristics of these three waveguides suggests that their excitation cross section values must be comparable despite the significant difference between crystalline qualities and losses. Note that this excitation cross section value is very similar to that measured for erbium ions in silica fiber previously reported.¹ This indicates that for resonant excitation, the cross section is relatively independent of the host material.

In conclusion, we have measured the spontaneous emission carrier lifetimes in Er:GaN waveguides of different losses and found that the carrier lifetime is directly related to the semiconductor crystalline quality of the waveguide. We have also identified the value of excitation cross section of Er:GaN at 980 nm pumping wavelength and found that this

excitation value of $2.2 \times 10^{-21} \text{ cm}^2$ is relatively insensitive to the crystalline quality.

The optical characterization work was supported by NSF (ECCS-1200168) and the materials growth effort was supported by JTO/ARO (W911NF-12-1-0330). Jiang and Lin acknowledge the AT&T Foundation for the support of Ed Whitacre and Linda Whitacre endowed chairs.

¹E. Desurvire, *Erbium-doped Fibre Amplifiers: Principles and Applications* (John Wiley & Sons, 1994).

²R. J. Mears, L. Reekie, I. M. Jauncey, and D. N. Payne, "Low noise erbium-doped fibre amplifier operating at 1.54 μm ," *Electron. Lett.* **23**, 1026 (1987).

³P. C. Becker, N. A. Olsson, and J. R. Simpson, *Erbium-Doped Fibre Amplifiers: Fundamentals and Technology* (Academic Press, 1999).

⁴M. J. Connelly, *Semiconductor Optical Amplifiers* (Springer, 2002).

⁵S. Xu, J. B. Khurgin, I. Vurgaftman, and J. R. Meyer, "Reducing crosstalk and signal distortion in wavelength-division multiplexing by increasing carrier lifetimes in semiconductor optical amplifiers," *J. Lightwave Technol.* **21**, 1474 (2003).

⁶H. Ishigawa, G. Y. Zhao, N. Nakada, T. Egawa, T. Soga, T. Jimbo, and M. Umeno, "High-quality GaN on Si substrate using AlGaIn/AlN intermediate layer," *Phys. Status Solidi A* **176**, 599 (1999).

⁷J. Li, J. Y. Lin, and H. X. Jiang, "Growth of III-nitride photonic structures on large area silicon substrates," *Appl. Phys. Lett.* **88**, 171909 (2006).

⁸R. G. Wilson, R. N. Schwartz, C. R. Abernathy, S. J. Pearton, N. Newman, M. Rubin, T. Fu, and J. M. Zavada, "1.54 μm photoluminescence from erbium and oxygen co-implanted GaN," *Appl. Phys. Lett.* **65**, 992 (1994).

⁹M. Garter, J. Scofield, R. Birkhahn, and A. J. Steckl, "Visible and infrared rare-earth-activated electroluminescence from indium tin oxide Schottky diodes to GaN:Er on Si," *Appl. Phys. Lett.* **74**, 182 (1999).

¹⁰J. M. Zavada, S. X. Jin, N. Nepal, H. X. Jiang, J. Y. Lin, P. Chow, and B. Hertog, "Electroluminescent properties of erbium-doped III-N light-emitting diodes," *Appl. Phys. Lett.* **84**, 1061 (2004).

¹¹R. Dahal, C. Ugolini, J. Y. Lin, H. X. Jiang, and J. M. Zavada, "Erbium-doped GaN optical amplifiers operating at 1.54 μm ," *Appl. Phys. Lett.* **95**, 111109 (2009).

¹²I-W. Feng, J. Li, J. Lin, H. Jiang, and J. Zavada, "Optical excitation cross section of erbium in GaN," *Appl. Opt.* **52**(6), 1132–1135 (2013).

¹³I-W. Feng, W. Zhao, J. Li, J. Lin, H. Jiang, and J. Zavada, "Correlation between the optical loss and crystalline quality in erbium-doped GaN optical waveguides," *Appl. Opt.* **52**(22), 5426–5429 (2013).

¹⁴Q. Wang, R. Hui, R. Dahal, J.-Y. Lin, and H.-X. Jiang, "Carrier lifetime in erbium-doped GaN waveguide emitting in 1540 nm, wavelength," *Appl. Phys. Lett.* **97**, 241105 (2010).

¹⁵F. Priolo, G. Franzò, S. Coffa, and A. Carnera, "Excitation and nonradiative deexcitation processes of Er^{3+} in crystalline Si," *Phys. Rev. B* **57**(8), 4443–4455 (1998).